Magazine of Civil Engineering

ISSN 2712-8172

journal homepage: http://engstroy.spbstu.ru/

DOI: 10.18720/MCE.100.5

Distribution of corrosion products at the steel-concrete interface of XD3 concrete samples

S.A. Abdulsada*, F. Kristaly, T.I. Torok
University of Miskolc, Miskolc, Hungary
** E-mail: qkosha86@uni-miskolc.hu*

Keywords: reinforced concrete, green inhibitor, superplasticizers, X Ray Diffraction, corrosion.

Abstract. This research paper deals with the steel/concrete interface of concrete samples with and without green inhibitor (orange peel extract) and with different two types of superplasticizers (Mapei Dynamon SR 31 and Oxydtron) after an 18 months exposure in aqueous chloride environment. XRD, SEM, and light optical micrograph techniques were applied to investigate the chemical compositions and the spatial distribution of the corrosion products. The experimental results revealed and illustrate that the corrosion products were visible in samples without inhibitor and appeared less noticeable in samples with Mapei Dynamon SR 31 but in the samples with Oxydtron were almost non-existent.

1. Introduction

As it is stated in many relevant publications, the corrosion of steel reinforcement is a major problem influencing the long-term performance of reinforced concrete structures. It typically occurs due to onslaught of aggressive agents such as chloride ions from marine environment, dicing salt or chloride contaminated aggregate [1–3]. One of exposure classification for reinforced concrete according to EN 1992-2 [4] was XD3 and the corrosion for this class induced by chlorides other than from seawater and it be Cyclic wet and dry, this exposure may occur in parts of bridges exposed to spray containing chlorides, pavements, car park slabs. In presence of chloride, these ions are known to be able to locally damage passivating films on metals and alloys that exhibit complete passivity against many natural environments in their absence (as shown in Fig. 1). The formation of corrosion products (rust) involves a substantial volume increase, i.e. the volume of corrosion products is greater than that of original steel bar. Therefore, expansive stresses are induced around corroded steel bars causing possible cracking, spalling of concrete cover and loss of bond between the steel and the concrete matrix and thus reducing the serviceability of steel reinforced concrete structures [5–11].

Cracking of the concrete cover is a critical limit state and this is often modelled as a two-stage process that consists of a) an initiation phase, defined as the time taken for corrosion to commence, and b) propagation phase, where the accumulation of corrosion products induces expansive stresses and damage [12–14].

Anyhow, as a preventive measure against steel rebar corrosion, it is highly recommended by many corrosion experts [e.g. 16–19] studying the mechanism of the reinforcing steel corrosion in concretes, that inhibitors added to the fresh concrete mixtures can effectively defer the initiation phase of corrosion as well as decrease its rate during the propagation phase.

As it is well known, the corrosion inhibitors are chemical substances that when added in small amount to concrete mix decrease or slow down corrosion rate by changing the surface condition of the reinforced steel [20]. Most of the corrosion inhibitors are classified as organic and inorganic ones according to their chemical nature as well as anodic, cathodic or mixed inhibitors according to the electrochemical reaction on the steel surface with its environment [21].

Abdulsada, S.A., Kristaly, F., Torok, T.I. Distribution of corrosion products at the steel-concrete interface of XD3 concrete samples. Magazine of Civil Engineering. 2020. 100(8). Article No. 10005. DOI: 10.18720/MCE.100.5

 This work is licensed under a CC BY-NC 4.0

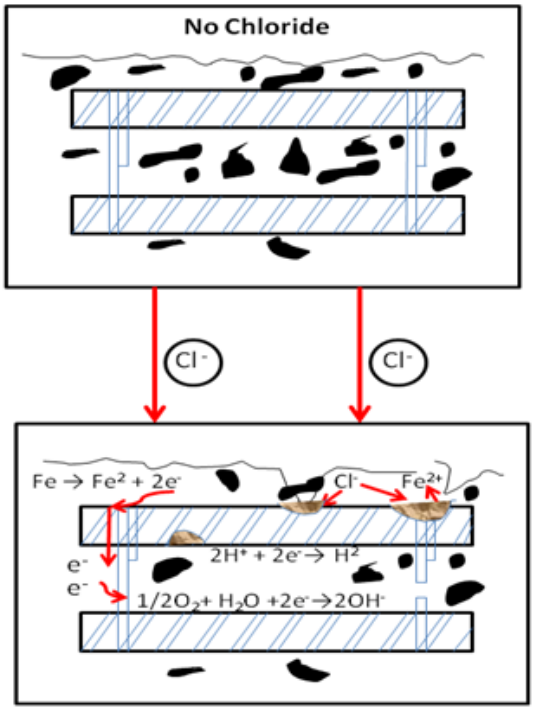

Figure 1. Electrochemical corrosion processes triggered by Cl⁻ ions reaching reinforcements, (modified from [11]).

The main purpose of this paper is to present an experimental study pursued by SEM-EDS, XRD analysis and light optical microscopy to monitor and evaluate corrosion products at the steel-concrete interface of XD3 concrete with green inhibitor and two types of superplasticizers.

2. Methods

2.1. Materials and Experimental work

2.1.1. Materials Used

All materials were used in this work conformed to the European Standards starting with cement (Portland slag cement CEM II/A-S 42.5R conforming to the EN 197-1 [22]) and then aggregates (fine and coarse according standard EN 12620 [23]). Steel rebar samples selected with diameter of 8 mm for this work. Tap water was used for both making and curing the specimens. Used three types from admixtures during preparing concrete samples, one of these admixtures was orange peels extract as a green inhibitor (this inhibitor was selected because it cheap, not harmful and eco-friendly as we mention it in previous published work [1, 2]), the other two admixtures were Mapei Dynamon SR 31 and Oxydtron (nanocement) as a superplasticizers.

2.1.2. Samples Preparation

The European mix design method type XD3 class was used to preparing concrete mixes. The cover depth of concert we select the structure class type S2 with depth 35mm have service life of 10 to 25 years according to the EN 1990 [24]. The composition of the mix prepared for casting the specimens was as follows:

Cement: 400 kg/m^3 (CEM II/A-S 42.5 R), Water: 172 kg/m^3 (w/c = 0.43 planned/targeted value).

Admixtures: 2.4 kg/m^3, Additive: 1815 kg/m^3 [(sand 0/4: 60 % 1089 kg/m^3) and (gravel 4/8: 40 % 726 kg/m^3)].

Mass percentages of the two special additives compared to the amount of cement type CEM II/A-S 42.5R for the prepared concrete samples are given in Table 1. The samples had been immersed and kept in 3.5 % NaCl solution for 18 months then the samples were removed from the 3.5 % NaCl solution as shown in Figs. 2, 3.

Table 1. The concrete mixtures (specimens) prepared for this study.

Type of Mixtures		
Symbol of Mix	Type of Admixture	Concentration of Green Inhibitor
A1 (Reference)	MapeiDynamon SR 31	without
B1	MapeiDynamon SR 31	1% byweight of cement
C1	MapeiDynamon SR 31	3% byweight of cement
A2 (Reference)	Oxydtron	without
B2	Oxydtron	1% byweight of cement
C2	Oxydtron	3% byweight of cement

Figure 2. Reinforced concrete samples were immersed in 3.5 % NaCl solution for 18 months.

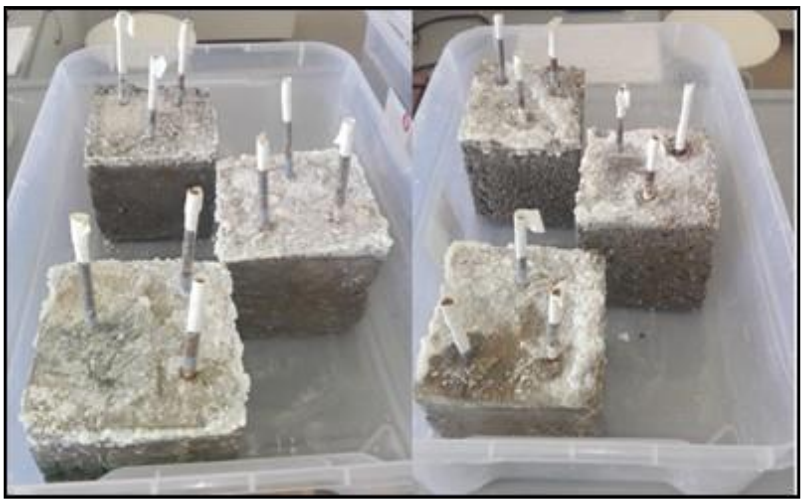

Figure 3. Reinforced concrete samples removed after 18 months immersion in 3.5% NaCl solution.

After drying, the concrete cubes/blocks (15 cm×15 cm) were cut into several parts as shown in Fig.4 after that the steel rebar were taken out from the cubes.

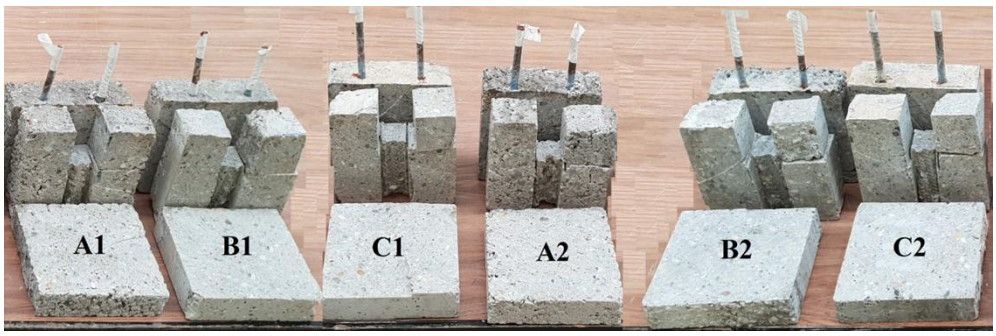

Figure 4. Reinforced concrete samples after cutting and removing one reinforcing steel bar from each sample.

2.2. SEM observation

It is well-known that not all corrosion products participate in concrete cracking as some of them fill in the voids around the rebars and some of them migrate from the steel/concrete interface to the pores in concrete. Scanning electron microscopy (SEM) imaging and EDS elemental mapping were employed on the surface of the steel rebars after detaching them from the concrete blocks in order to assess spatial distribution of corrosion products at the steel/concrete interface. Measurements were done on Zeiss EVO/MA10, using accelerating voltage of 15 kV.

2.3. Optical microscopy

Thin sections (thickness 1cm) were also cut from each sample to examine with light optical microscopy. The cut sections were dried in air, impregnated with epoxy resin under vacuum, and finally grounded and polished by silicon carbide papers of up to 1200 grit; 6-mm and 3-mmdiamond spray and finally, 0.05-mmAl_2O_3 suspension, etched (in 3 % Nital, for approximately 10 s). In this study, light optical microscopy was especially used to detect the extent and spatial distribution of rust, capillary porosity and secondary precipitated phases in voids and cracks at the steel-concrete interface of the samples.

2.4. XRD analysis

To clarify the rust compositions and diffusion of water and chloride ions, small concrete parts were sampled from the concrete in direct contact with the steel bars as shown in Fig. 5. These parts were then ground and analyzed by powder X-ray diffraction (XRD). The powder samples (size < 5 μm) were analyzed by the XRD technique using CuKα-radiation at angles from 2θ = 2º to 70º (0.007°2 θ/24 sec counting time) on a Bruker D8 Advance instrument, in parallel beam geometry obtained with Göbel mirror, equipped with Vantec-1 position sensitive detector (1° opening).

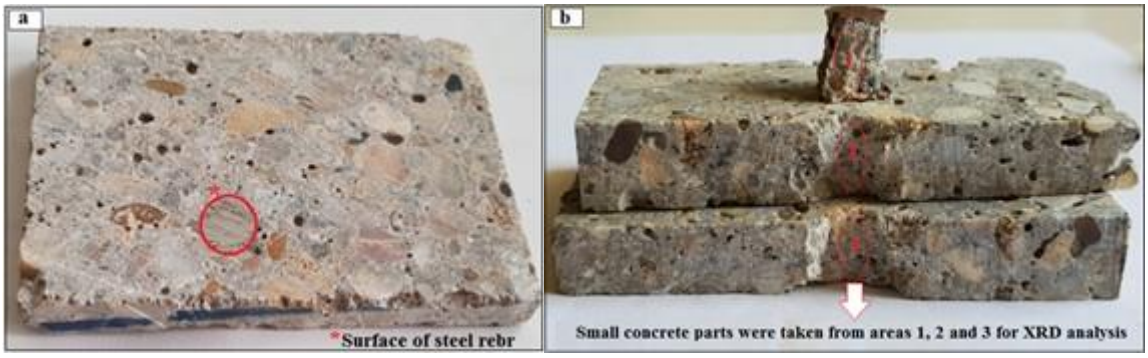

Figure 5. Concrete samples after cut and prepared for XRD analysis, a) before cut, b) after cut and removed the steel rebar.

3. Results and Discussion

3.1. SEM-EDS Microstructural and Composition Analysis of the Steel Rebar Surface

For the microstructural SEM investigations the steel rebar specimens/rods first had to be removed from the concrete blocks which had previously been kept immersed in 3.5%NaCl solution for 18 months. After that the SEM-EDS analysis could be commenced and the results are presented in Fig. 6. The chemical elementary compositions determined at some selected surface points on the steel rebars (as marked clearly in Figure 6) were obtained by the EDS method being coupled to the scanning electron microscope (SEM) and are given in wt% in Table 2.

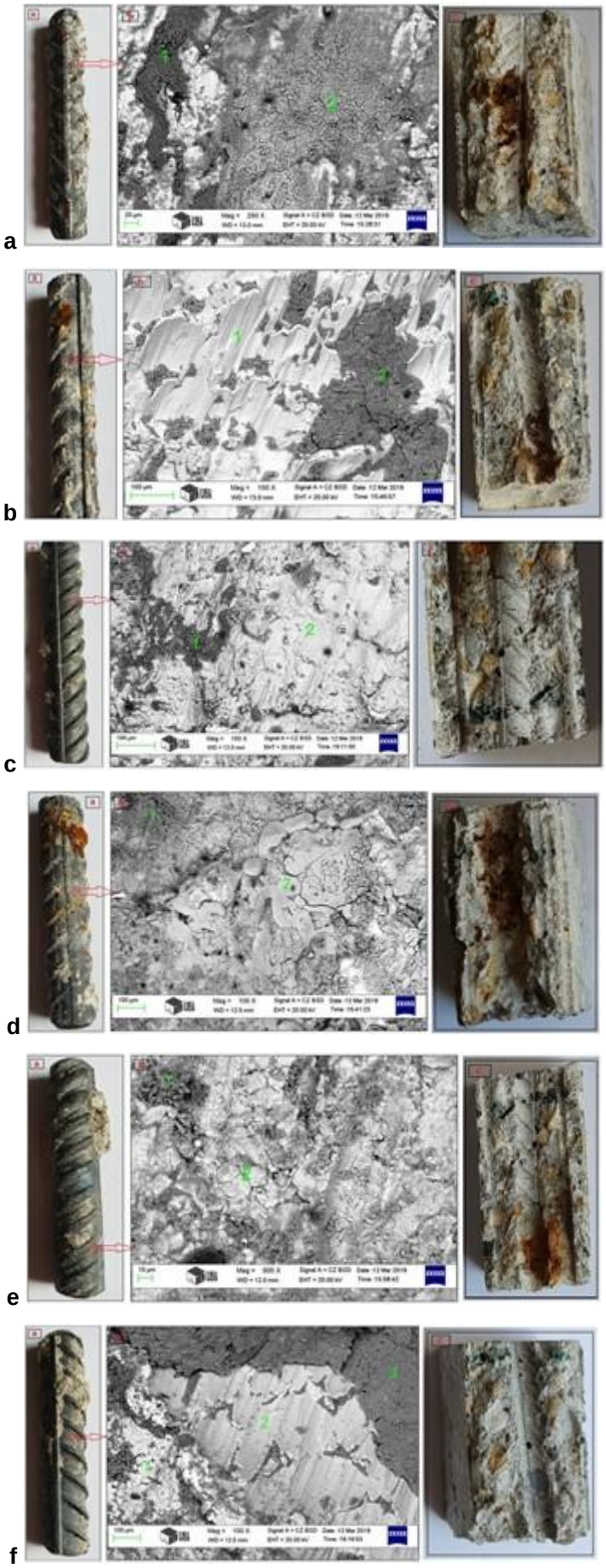

Figure 6. a) Close-up image of a steel rebar for sample: a) A1, b) B1, c) C1, d) A2, e) B2, f) C2, after removal from the concrete, b) SEM Micrograph of the section indicated in (a), c) Representative image of a split concrete specimen after removal of the steel rebar.

Table 2. The approximate chemical composition (expressed as oxides) of some small selected surface areas (as indicated in Fig. 6) of the steel rebars after removal from the concrete blocks by SEM-EDS

Components (as Oxides)	Composition by EDAX (ZAFcorrection) given in wt%, not normalised												
	A1		B1		C1		A2		B2		C2		
	Point 1	Point 2	Point 1	Point 2	Point 1	Point 2	Point 1	Point 2	Point 1	Point 2	Point 1	Point 2	Point 3
Na_2O	0.13	0.46	3.61	1.38	2.36	1.40	0.14	0.35	13.61	6.01	3.61	6.45	0.61
MgO	0.00	0.30	1.42	4.13	2.29	2.26	1.16	0.25	3.13	2.31	3.15	0.50	4.28
Al_2O_3	0.19	0.95	1.21	10.9	5.62	1.22	1.26	0.59	2.35	1.32	2.39	0.57	2.77
SiO_2	1.38	2.01	3.41	17.6	24.7	10.7	0.59	1.07	10.6	7.80	10.6	3.11	16.7
SO_3	1.04	0.55	1.10	5.75	4.93	2.28	0.23	0.28	0.58	0.38	0.58	7.39	2.18
Cl_2O	3.51	0.23	1.83	0.68	3.98	0.31	5.10	2.06	0.24	0.11	0.20	1.90	0.91
K_2O	0.11	0.16	0.98	0.84	0.96	1.25	0.10	0.07	0.45	0.17	0.5	1.75	0.54
CaO	0.51	2.54	9.65	52.6	40.4	21.1	1.00	0.84	39.2	15.5	39.2	16.0	58.4
MnO	0.91	0.87	0.83	0.67	0.72	1.08	0.09	0.15	2.79	1.68	2.79	0.66	0.71
FeO	92.2	91.9	75.9	5.32	2.36	55.4	92.3	94.3	47.1	64.7	37.1	61.7	12.9

Fig. 6a represents the reinforcing steel specimen for sample A1, which showed an oxidized surface state (small oxidized areas spread over most of the specimen surface) and its composition was found similar to that of pure FeO as it contained about 92.23 wt% FeO at point 1 and 91.93 wt% at point 2. It is seen from Table 2 at point 2 that at the steel surface of the same sample A1 also some compound-bound chlorine (expressed as Cl_2O of 3.51wt%) could be detected, which indicates that the chloride ions migrated in wards and could reach the surface of steel rebar. As this concrete sample did not contain any corrosion inhibitor (namely the orange peel extract), the chloride ions could diffuse easily and fast to the steel surface and even initiate and/or enhance its corrosion with the probable later formation of different iron-oxide-hydroxide(rust) compounds, although the marked and EDS tested two points may also be related to the original mill-scale coverage of the steel bars received directly from a reinforcing steel rod producer and studied also by use earlier [2, 3]. Anyhow, the presence of chlorine observed right at the steel/concrete interface is a strong indication of the chloride ion ingress reaching to the rebars surface also at some other samples (see in Table 2) after 18 months immersion in the given aqueous chloride salts solution.

Figure 6b shows the steel rebar specimen in sample B1 that presents a little bit oxidized area on the surface but at the spot that was selected for testing and is marked as point 1 had FeO in 75.97wt%, which means this point(s) were attacked by pitting corrosion due probably to the rather low concentration of the green inhibitor (1 %) that could not prevent the break down of the thin passive surface oxide layer. Hence, at some “weakest points” this protective layer could be „destroyed” (i.e. chemically modified and dissolved away) from the steel surface due primarily to the attack of chloride ions (given as Cl_2O of 1.83 wt%) which could reach the surface of steel as shown in Table 2 at point 1 of B1.

In Fig. 6c the surface of the reinforcing steel in sample C1 appears almost free of oxidation, but in the micro-structure analysis test made by EDS it showed FeO in ~66.06wt%, and CaO ~15.45 wt% at point 2 and in the same point it also had some chlorine (expressed in $Cl_2O$of about 0.31 wt%), so these oxides not only as a rust in this point but also came from concrete composition.

From Fig. 6d can note the effect of chloride on the surface of steel rebar in sample A2 because it has oxidized areas clear and widespread on the surface (FeO ~ 92.33 wt%, at point 1 and 94.34 wt%, at point 2). This sample has no ability to resist the corrosion and the amount of chloride ions that reached to the surface of steel its high (Cl_2O ~ 5.10 wt% at point 1 and 2.06 wt% at point 2) and this quantity consider risk and the probability of corrosion its high also.

Fig. 6e represents the steel rebar in sample B2 had only in micro-structure by EDAX test a little bit oxidized composition but it does not appear clearly on the surface (FeO ~ 64.74 wt% at point 2), also the amount of chlorides in this sample not high as shown in Table 2 at point 2.

In Fig. 6f the reinforcing steel in sample C2 considers the best one because it had a very little bit oxide areas and this oxide is not appeared on the surface of steel only detected by EDAX test compare with other samples, it means that there is a very low probability to corrosion risk in this sample.

The observed micro-structure by SEM technique features (presented in Fig. 6) and the EDS analysis for composition (Table 2) indicate the effects of the changing bulk and boundary materials properties, like the porosity and pore solution, as well as alterations at the metal/solution interfaces inside the concrete samples being immersed up to 18 months in 3.5 % NaCl solution. In this respect our observations are in harmony with those of some other researchers [25, 26] having dealt with somewhat similar systems and explained the observed phenomena by the formation of porous corrosion products modifying the charge transfer resistance at the steel/solution interface.

The increases in the corrosion (by formation oxidized area) can mainly be related to the structural consequences of the hydration processes (so-called hardening) of the concrete bodies, that is the liberation of calcium hydroxide, $Ca(OH)_2$, and/or the formation of the well known cementitious compounds C3S or C3A, etc. The tested two admixtures (Oxydtron /nanocement/ and Mapei Dynamon SR 31) added to the fresh concrete during the preparation step of the samples gave rise to reducing the water/cement ratio during the concrete blocks hardening, therefore there was not enough time for the formation of $Ca(OH)_2$ and/or C3S and/or C3A, .. etc. (which compounds cause greater capillary porosity in concrete and weakens the properties). While discussing the topic of the so-called nanocement admixtures as well, Yakub et al. [27] described some relevant details of the so-called pozzolanic reaction of vitreous silica with calcium hydroxide ($Ca(OH)_2$ also abbreviated as (C–H). During this hydration reaction of the Ordinary Portland Cement (OPC) this binder is producing additional calcium silicate hydrate (C–S–H) that resembles tobermorite or jennite structure, which is the main constituent for providing the strength and density in the hardening binder paste. The pozzolanic activity includes two parameters; the amount of lime ($Ca(OH)_2$) that pozzolan can react with it and the rate of reaction. The rate of the pozzolanic activity is related to the surface area of pozzolan particles where higher surface area of pozzolan particle (or finer particle) gives more pozzolanic reactivity. And, due to the very high specific surface area and the spherical particle shape of the synthetic nanosilica admixture, it can potentially enhance the performance of binder mainly due to its reaction with C–H to develop more of the strength-carrying compound in binder structure: C–S–H [27]. Hence, just by analogy, it can be stated with high probability, that the Oxydtron (nanocement) admixture should also behave in a somewhat similar fashion to that of the nanosilica admixture.

Nevertheless, the admixture Oxydtron did reduce the ratio of water/cement less than Mapei Dynamon SR 31, which means that the capillary porosity in the structure of the concrete body is higher than with SR 31. So after adding the green inhibitor (especially in 3 % as in C2 sample) to the fresh concrete, this inhibitor can and will work as a retarder, i.e. it retards the action of $Ca(OH)_2$ and/or C3S and/or C3A and also will diffuse through the pores and give a more closed structure of the samples. And so, eventually it will provide the samples better resistance against chloride diffusion and the concrete will be more resistant to steel rebar corrosion.

Usually, chloride ions cannot penetrate enough deep into the concrete within short time. However, after a long time in chloride ions containing environment chloride ions can arrive to and accumulate in a sufficiently high concentration at the metallic surface of the steel rebar in the concrete samples to initiate corrosion. This behavior is mainly due to distortion of passive layer (caused by the green inhibitor) on the surface of reinforced steel in agreement with the observations of the researchers Magdy A. et al. [28].

3.2. Optical Microscopy

Light optical micrograph for all concrete samples is presented in Fig. 7.

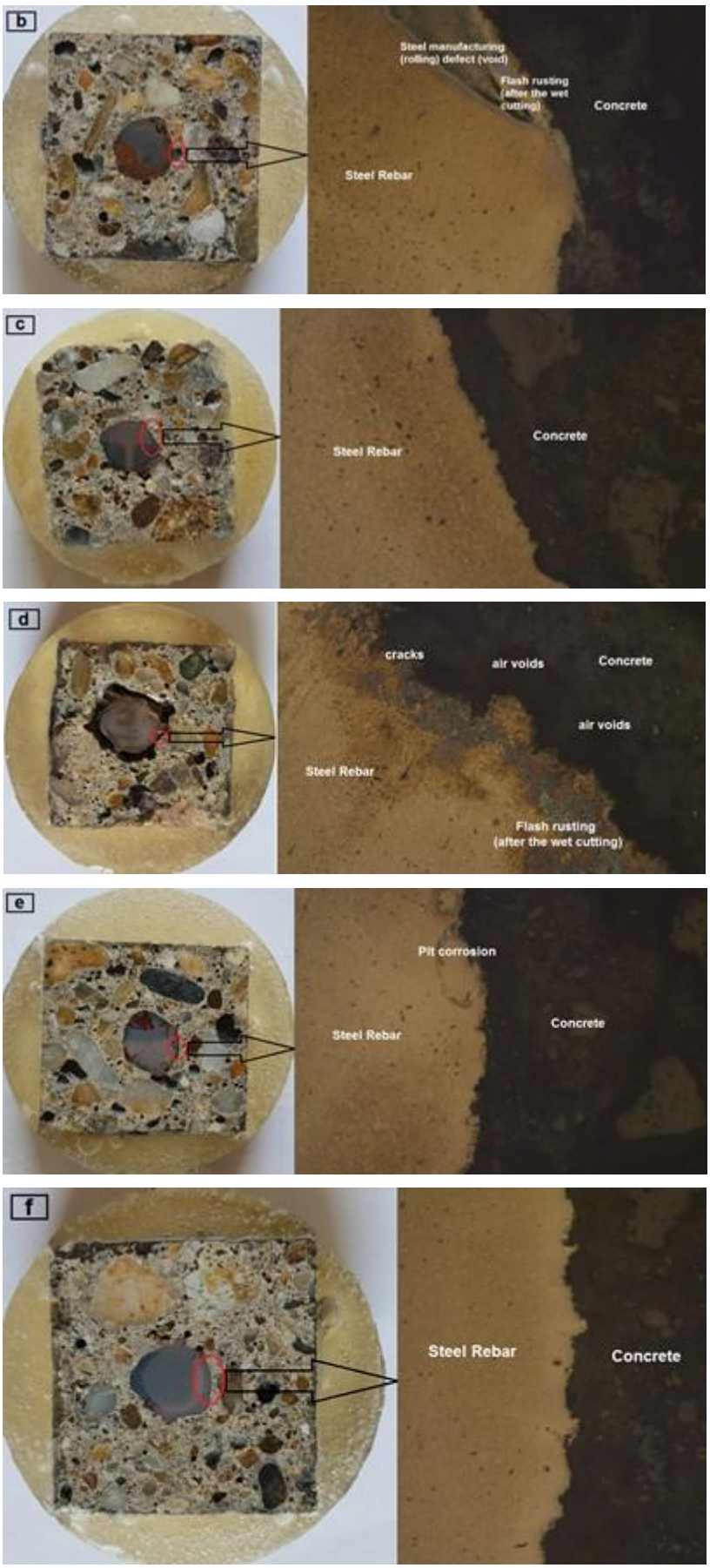

Figure 7. Light optical micrograph of the steel-concrete interface section with magnification 50X of the sample: a) A1, b) B1, c) C1, d) A2, e) B2, f) C2, showing the microstructure and the corrosion attack.

The visual examination revealed that in 75 % of all cases, corrosion initiated between the rebar ribs or directly at the rib edge as shown in Fig. 7a,d (samples A1 A2) and the type of corrosion as a flash rusting (after wet cutting for samples), also the cracks and air void appeared in theses samples.

Fig. 7b (sample B1) illustrates there's a steel manufacturing (rolling) defect (void) and small a flash rusting (after wet cutting for samples) areas.

Inspection of the steel-concrete interface upon corrosion initiation typically revealed the presence of one distinct corroding spot, which in some cases was surrounded by significantly smaller corrosion pits, all of them within an area of maximum approximately 1 mm^2 as shown in Fig. 7e (samples B2). The small corrosion pits were interpreted as sites where corrosion had initiated but was not able to reach stable pit growth (in contrast to the dominating corrosion site), these pits were typically covered with a crust of corrosion products, which occasionally remained even after the chemical cleaning process in inhibited hydrochloric acid.

Inspection of the samples C1 and C2 (Fig. 7c,f) showed there is no pits corrosion or cracks at the steel-concrete interface.

3.3. Composition analysis of corrosion products by XRD test

In Fig. 8 all the XRD records measured for the concrete samples at their steel-concrete interfaces are collected and presented from a) to f).

X-ray diffraction measurements detected the same products (Portlandite very low content and abundant content from calcite plus corrosion products (Brownmillerite, Biotite, Muscovite, Hydrocalumite, Ettringite, Chlorite) middle content), in concrete at its interface with concrete, as for free inhibitor samples. But the amount of calcite is lower and low or very low content amount of corrosion products in concrete samples containing inhibitor (samples with 1 %, 3 % green inhibitor) than in the other specimens. Amorphous material was also detected, and is a product of corrosion and is made up by Fe-oxyhydroxides („rust") and Ca-Al-silicate hydrates.

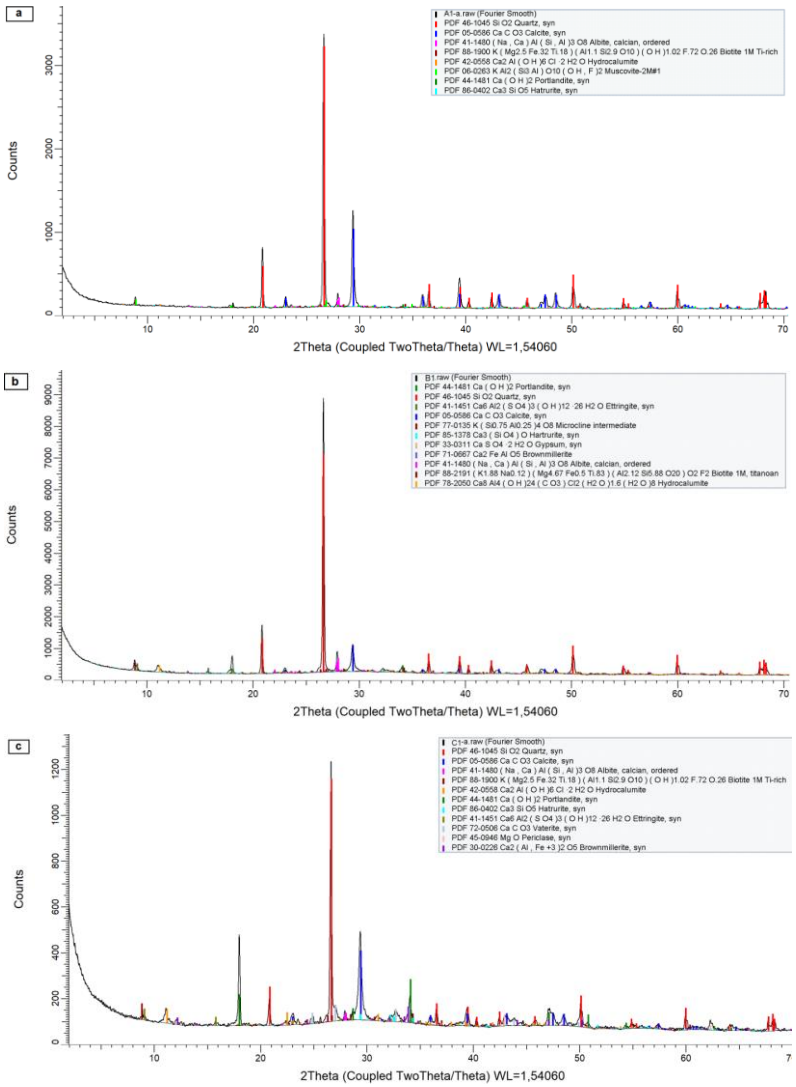

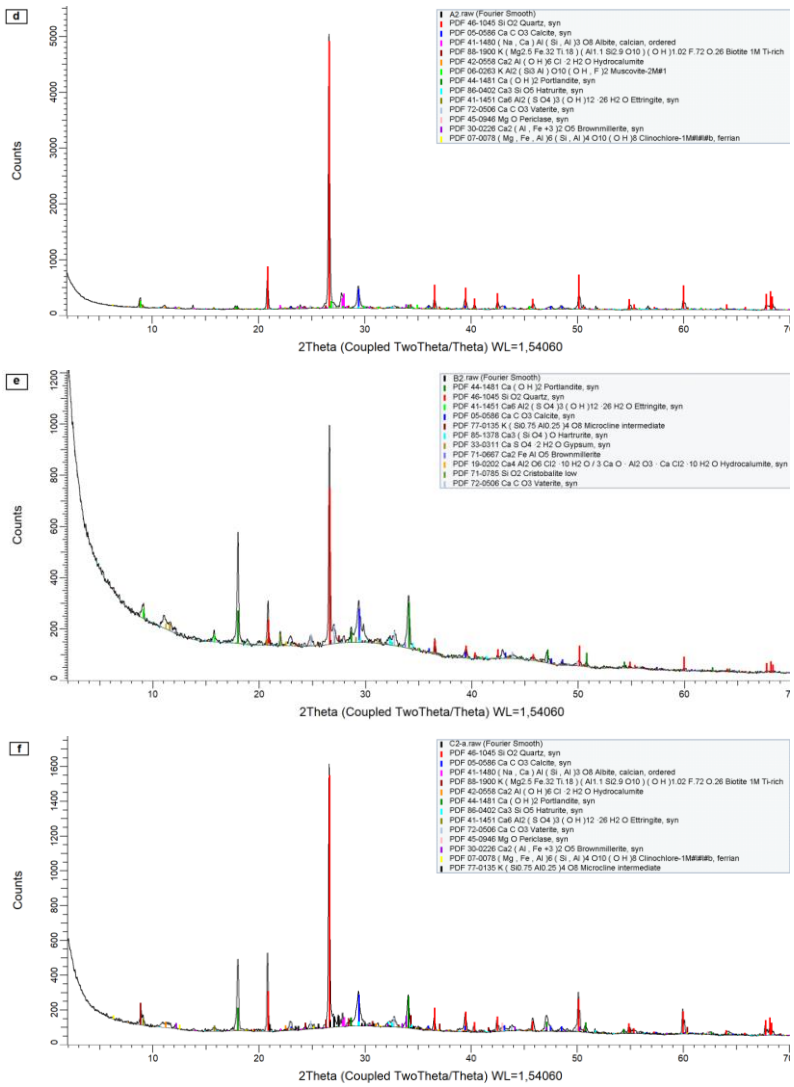

Figure 8. XRD pattern of corrosion products in the interface between steel and concrete for sample: a) A1, b) B1, c) C1, d) A2, e) B2, f) C2, after immersion in 3.5% NaCl for 18 months.

Table 3. The qualitative content of the main crystalline hydration products in samples at concrete-steel interface by XRD analysis.

Compound name with formula	Qualitative content of compounds					
	A1	B1	C1	A2	B2	C2
Portlandite [$Ca(OH)_2$]	+	+++	+++	+	+++	++++
Calcite [$CaCO_3$]	++++	+++	+++	++++	++	+++
Ettringite [$Ca_6Al_2(SO_4)_3(OH)_{12}\cdot 26H_2O$]	+++	+++	++	+++	+++	++
Hydrocalumite [$Ca_2Al(OH)_6Cl\cdot 2H_2O$]	+++	+	++	+++	++	+
Biotite [$K(Mg,Fe)_3(AlSi_3O_{10})(F,OH)_2$]	+++	+	+	++	+	+
Brownmillerite[$Ca_2(Al, Fe)_2O_5$]	+++	++	++	+++	+++	+
Muscovite [$KAl_2(AlSi_3O_{10})(FOH)_2$]	+++	No	No	+++	No	No
Chlorite[$(Mg,Fe,Al)_6(Si, Al)_4O_{10}(OH)_8$]	++	No	No	++	No	No

Notation: ++++: Abundant content; +++: Middle content; ++: Low content; +: Very low content; No: Absence.

The XRD pattern (Fig. 8) for all concrete samples (with and without inhibitors) demonstrates the presence of strong peak is Quartz (SiO_2, deriving from the sand grains in mortar) at about 2θ of 26.5°. The second clear and important peak is Portlandite ($Ca(OH)_2$) at 2θ = 18° and 34° was created by the hydration of calcium silicates. Calcium hydroxide quantity precipitated at the steel surface is important in resist effect of corrosion. The protective effect of calcium hydroxide was attributed to the dissolution of calcium hydroxide crystals close to emerging pits, thereby preventing the pH drop required for the further propagation of the corrosion pit [29].

Calcite ($CaCO_3$) of a small peak at 2θ of 29.5° is attributed to carbonation of hydrates on steel surface. The presence of these two last compounds can be explained by the fact that some traces of concrete materials could remain adhered to the rust during the sampling. Because all the samples were subjected to chloride ingress, the presence of Hydrocalumite ($Ca_2Al(OH)_6Cl{\cdot}2H_2O$) is justifiable and is confirmed by small peaks at 2θ = 11° and 21° in low and very low content for the samples with inhibitors and in middle content for samples without inhibitors. A little amount of Brownmillerite ($Ca_2(Al, Fe)_2O_5$), Biotite ($K(Mg,Fe)_3(AlSi_3O_{10})(F,OH)_2$), Muscovite ($KAl_2(AlSi_3O_{10})(FOH)_2$), Ettringite ($Ca_6Al_2(SO_4)_3(OH)_{12}{\cdot}26H_2O$), Chlorite ($(Mg,Fe,Al)_6(Si, Al)_4O_{10}(OH)_8$) as a corrosion products can be observed in different quantities in some of concrete samples as shown in Table 3 .

However, iron oxides (Hematite (Fe_2O_3) or Maghemite (γ-Fe_2O_3)) cannot be clearly distinguished by this XRD pattern because their diffraction patterns are amorphous phases, only Iron(II) oxide (FeO) we distinguished by SEM technique.

Sample C2 has portlandite in high quantity this can explain the resistance of these samples to the attack of chlorides and very little corrosion products because the electrochemical mechanism of pitting corrosion confirms the inhibitive nature of OH^- in the pore solution. The pH value of the pore solution in concrete is mainly maintained by the portlandite ($Ca(OH)_2$) from the cement hydration and the alkaline ions (Na^+, K^+) in the pore solution. The inhibitive effect of OH^- on pitting corrosion is enhanced by the concentrated distribution of $Ca(OH)_2$ on the concrete–steel interface. The quality of the concrete–steel interface conditions the electrochemical environment of the pitting corrosion: concentrated CH (calcium hydroxide) can effectively inhibit the initiation, while the air voids and cracks at the interface can favor the formation of macrocells and thus accelerate the initiation [30].

An increased amount of CH close to the steel in reinforced concrete as observed in this work may be beneficial, in that it may lead to improved local pH-buffering capacity and thus to better protection against carbonation-induced generalized corrosion; that is, it would take a longer time for the larger amount of CH near the interface to react to form calcium carbonate thus delaying the drop in pH associated with complete carbonation. However, it is possible that this potential benefit might not be realized in practice if the CH simply becomes encased in calcium carbonate whilst the surrounding C–S–H becomes completely carbonated, as has been observed in partially carbonated hardened cement pastes by transmission electron microscopy. Certainly, a partially carbonated zone that consists of completely carbonated C–S–H and regions of CH encased in calcium carbonate would seem to be a very plausible explanation for the observation of corroded steel in regions of concrete that appears 'uncarbonated' to the phenolphthalein test [31].

Samples A1, A2 has abundant content from calcite and because this component there's no ability to resist the effect of corrosion risk. Concrete carbonation due to atmospheric CO_2 is one of the main environmental aggression leading to steel corrosion. The high pH (13) of the concrete provides a natural protection against corrosion to the embedded reinforcement by forming a compact insoluble oxide film at the steel surface (passive state). But carbonation leads concrete pH to decrease to about 9 and active steel corrosion to start. Corrosion of steel in carbonated concrete is assumed to be uniform. In this case, anodic and cathodic areas form corrosion microcells which are not separated spatially, leading to a uniform steel loss.

In reinforced concrete structures, CO_2 penetration in the concrete cover is a complex process. Gradients in concrete humidity content affect a lot the carbonation rate, mechanical damage of concrete subjected to excessive tension can lead to a CO_2 penetration increase, the quality of the concrete cover (strength, porosity, permeability, etc.) can be very different in regard to the location in the structure.

Carbonation occurs in concrete because the calcium hydrates present are attacked by carbon dioxide of the air and converted to calcium carbonate (Eq. (1)), leading to a decrease in pH to about 9 and active steel corrosion can start [29]. The concrete will carbonate if CO_2 from air enters the concrete according to: $Ca(OH)_2+CO_2= CaCO_3+H_2O$ (1) [32]

The interface is regarded as a major factor in corrosion initiation. Since the pores and voids at the concrete-steel interface are not always saturated by pore solutions, the availability of oxygen (gas phase) and the pore solution (liquid phase) impact on corrosion initiation. Both are necessary to start up the cathodic reaction for corrosion. Accordingly, highly saturated and very dry concretes tend to have high resistance to chloride initiation of corrosion and the structural degradation of the concrete matrix [30].

4. Conclusion

While testing the steel rebar specimens after removal from the steel reinforced concrete blocks previously kept in aqueous salt solutions for 18 months and after analyzing their steel-concrete interfaces we can arrive to the following major concluding points:

1. Corrosion products (FeO, Cl_2O) was detected by SEM- EDAX on the surface of steel rebar after removal from concrete samples increase with decrease concentration of green inhibitor (orange peel extract) and the steel of sample C2 had the lowest rate from corrosion products in the points examined compared to the rest of the steel samples, this can also be seen from the external appearance of the steel surface as it is almost free from corrosion products because it has a strong passive layer.

2. Cracks, porosity, corrosion pits, and air voids clearly appeared at the steel-concrete interfaces of A1, A2 samples which were revealed by the light optical microscopy analysis. Such undesirable features were less observable in samples with Oxydtron+ (1 %, 3 % green inhibitor) and Mapei Dynamon SR 31 (only with 3 % green inhibitor).

3. High quantities of Portlandite and almost non-existent amounts of Hydrocalumite, Biotite, Brownmillerite, Muscovite, Chlorite were detected in the steel-concrete interfaces of B1, C1, B2, C2 samples (in particular with C2 sample) by the XRD analytical technique.

4. The concrete sample C2 (with 3 % green inhibitor and Oxydtron admixture) had lower concentration of infiltrated/ingresses Cl^- ions after immersion in 3.5 % NaCl solution for 18 months in comparison to the other samples. Also this sample sowed the best resistance to corrosion.

5. Acknowledgements

We would like to thank Mr. László Köteles, Institute of Mining and Geotechnical Engineering in Faculty of Earth Science and Engineering for cutting the concrete samples and Mr. Kovács Árpád, Institute of Physical Metallurgy, Metalforming and Nanotechnology, Faculty of Material Science and Engineering, both from University of Miskolc for the SEM+EDS measurements.

References

1. Shaymaa, A.A., Éva, F., Tamás, I.T. Corrosion testing on steel reinforced XD3 concrete samples prepared with a green inhibitor and two different superplasticizers. Materials and Corrosion. 2019. 70. Pp. 1–11. https://doi.org/10.1002/maco.201810695
2. Abbas, S.A., Török, T.I., Fazakas, É. Preliminary Corrosion Testing of Steel Rebar Samples in 3.5 % NaCl Solution with and without a Green Inhibitor. építőanyag-Journal of Silicate Based and Composite Materials. 2018. 70. Pp. 48–53. https://doi.org/10.14-382/epitoanyag-jsbcm.2018.10
3. Abbas, S.A., Török, T.I., Fazakas, É. Corrosion studies of steel rebar samples in neutral sodium chloride solution also in presence of a bio-based (green) inhibitor. International Journal of Corrosion and Scale Inhibition. 2018. 7. Pp. 38–47. http://dx.doi.org/10.17675/2305-6894-2018-7-1-4
4. EN 1992-2 (2005) (English): Eurocode 2: Design of concretestructures - Part 2: Concrete bridges - Design and detailingrules [Authority: The European Union Per Regulation305/2011, Directive 98/34/EC, Directive 2004/18/EC.
5. Shaymaa, A.A., Tamás, I.T. Measurements and Studying Corrosion Potential of Reinforced Concrete Samples Prepared with and without a Green Inhibitor and Immersed in 3.5 % NaCl Solution. MultiScience – XXXII. microCAD International Multidisciplinary Scientific Conference. University of Miskolc. 5–6 September, 2018. http://dx.doi.org/10.26649/musci.2018.014
6. El-Reedy, M.A. Steel-Reinforced Concrete Structures: Assessment and Repair of Corrosion, Second Edition. CRC Press, Taylor & Francis, London, 2018.
7. Quraishi, M.A., Nayak, D.K., Kumar, R., Kumar, V. Corrosion of Reinforced Steel in Concrete and Its Control: An overview. Journal of Steel Structures & Construction. 2017. 3. Pp. 1–6. https://doi:10.4172/2472-0437.1000124
8. Shaymaa, A.A., Ali, I.A., Ali, A.H. Studying the Effect of Eco-addition Inhibitors on Corrosion Resistance of Reinforced Concrete. Bioprocess Engineering. 2017. 1. Pp. 81–86. http://doi: 10.11648/j.be.20170103.14
9. Abosrra, L., Ashour, A.F., Youseffi, M., Corrosion of Steel Reinforcement in Concrete of DifferentCompressiveStrengths. Journal of Construction and Building Materials. 2011. 25. Pp. 3915–3925. https://doi.org/10.1016/j.conbuildmat.2011.04.023
10. Bertolini, L., Elsener, B., Pedeferri, P., Redaelli, E., Polder, R.B. Corrosion of Steel in Concrete: Prevention, Diagnosis, Repair, 2nd Edition. Wiley, New York, 2014.
11. González, J.A., Otero, E., Feliu, S., Bautista, A., Ramírez, E., Rodríguez, P., López, W. Some considerations on the effect of chloride ions on the corrosion of steel reinforcements embedded in concrete structures. Magazine of Concrete Research. 1998. 50. Pp. 189–199. https://doi.org/10.1680/macr.1998.50.3.189
12. Kim, M.J., Ann, K.Y. Corrosion Risk of Reinforced Concrete Structure Arising from Internal and External Chloride. Advances in Materials Science and Engineering. 2018. Pp. 1–7. https://doi.org/10.1155/2018/7539349
13. Faiz, A.S. Effect of Cracking on Corrosion of Steel in Concrete, International Journal of Concrete Structures and Materials. 2018. https://doi.org/10.1186/s40069-018-0234-y
14. Ming, J., Song, G., Linhua, J., Yu, J., Dan, W., Ruitong, S., Yirui, W., Junqiao, H. Continuous Monitoring of Steel Corrosion Condition in Concrete Under Drying/Wetting Exposure to Chloride Solution by Embedded MnO_2 Sensor. International Journal of Electrochemical Science. 2018. 13. Pp. 719–738. https: //doi.org /10.20964/2018.01.92
15. Wong, H.S., Karimi, A.R., Buenfeld, N.R., Zhao, Y.X., Jin, W.L. Microstructure of corroded steel-concrete interface 2012. On the web: http://www.imperial.ac.uk/structural-engineering/research/structural-materials/microstructure/
16. Zhao, Y.X., Karimi, A.R., Wong, H.S., Hu, B.Y., Buenfeld, N.R., Jin, W.L. Comparison of Uniform and Non-uniform Corrosion Induced Damage in Reinforced Concrete Based on a Gaussian Description of the Corrosion Layer. Corrosion Science. 2011. 53. Pp. 2803–2814. https://doi.org/10.1016/j.corsci.2011.05.017
17. Sagoe-Crentsil, K.K., Glasser, F.P. Steel in Concrete: Part I. A Review of the Electrochemical and Thermodynamic Aspects. Magazine of Concrete Research. 1989. 41. Pp. 205–212. https://doi.org/10.1680/macr.1989.41.149.205

18. Glasser, F.P., Sagoe-Crentsil, K.K. Steel in Concrete: Part II. Electron Microscopy Analysis, Magazine of Concrete Research. 1989. 41. Pp. 213–220. https://doi.org/10.1680/macr.1989.41.149.213
19. Sagoe-Crentsil, K.K., Glasser, F.P. Green Rust, Iron Solubility and the Role of Chloride in the Corrosion of Steel at High pH. Cement and Concrete Research. 1993. 23. Pp. 785–791. https: //doi.org /10.1016/0008-8846(93)90032-5
20. Burubai, W., Dagogo, G., Comparative Study of Inhibitors on the Corrosion of Mild Steel Reinforcement in Concrete. Agricultural Engineering International: the CIGR Ejournal. 2007. 9. Pp. 1–10.
21. Mahdi, A.S. Urea Fertilizer as Corrosion Inhibitor for Reinforced Steel in Simulated Chloride Contaminated Concrete Pore Solution. International Journal of Advanced Research in Engineering and Technology. 2014. 5. Pp. 30–39.
22. EN 197-1, Cement-Part 1: Composition, specifications and conformity criteria for common cements, European Standard was Approved by CEN National Members on 21 May 2000.
23. EN 12620, Aggregates for Concrete, European Standard was Approved by CEN National Members on September 2002.
24. EN 1990, Eurocode – Basis of structural design, European Standard was approved by CEN on 29 November 2001.
25. Mahallati, E., Saremi, M. An assessment on the mill scale effects on the electrochemical characteristics of steel bars in concrete under DC-polarization. Cement and Concrete Research. 2006. 36(7). Pp. 1324–1329. https://doi.org/10.1016/j.cemconres.20-06.03.015
26. Nielsen, A.H., Hvitved, T., Vollertsen, J. Effect of Sewer Headspace Air-Flow on Hydrogen Sulfide Removal by Corroding Concrete Surfaces. Water Environment Research. 2012. 84(3). Pp. 265–273. https://doi.org/10.2175/106143012X13347678384206
27. Yakub, I., Sutan, N.M., Kiong, C.S. Characterization of calcium silicate hydrate and calcium hydroxide in nanosilica binder composites. Nano Studuies. 2013. 7. Pp. 57–62. https://www.researchgate.net/publication/263738702_Characterization_of_calcium_silicate_hydrate_and_calcium_hydroxide_in_nanosilica_binder_composites
28. Magdy, A.A., Waleed, H. S., Effect of sewage wastes on the physico-mechanical properties of cement and reinforced steel. Ain Shams Engineering Journal. 2013. 4(3). Pp. 391–387. https://doi.org/10.1016/j.asej.2012.04.011
29. Sandberg, P. The effect of defects at the steel – concrete interface, exposure regime and cement type on pitting corrosion in concrete. (Report TVBM; Vol. 3081). Division of Building Materials, LTH, Lund University. 1998. https://portal.research.lu.se/portal/en/publications/the-effect-of-defects-at-the-steel--concrete-interface-exposure-regime-and-cement-type-on-pitting-corrosion-in-concrete(fa981216-1745-49c7-b73b-f6d7e03659ca).html
30. Kefei, li. Durability Design of Concrete structures, 1st edition. John Wiley & Sons, Singapore Pte. Ltd., 2016.
31. Horne, A.T., Richardson, I.G., Brydson, R.M.D. Quantitative analysis of the microstructure of interfaces in steel reinforced concrete. Cement and Concrete Research. 2007. 37. Pp. 1613–1623. https://doi.org/10.1016/j.cemconres.2007.08.026
32. Nasser, A., Clément, A., Laurens, S., Castel, A. Influence of steel–concrete interface condition on galvanic corrosion currents in carbonated concrete. Corrosion Science. 2010. 52. Pp. 2878–2890. https://doi.org/10.1016/j.corsci.2010.04.037

Contacts:

Shaymaa Abbas Abdulsada, qkosha86@uni-miskolc.hu
Ferenc Kristaly, askkf@uni-miskolc.hu
Tamas I. Torok, fektt@uni-miskolc.hu

© Abdulsada, S.A.,Kristaly, F.,Torok, T.I., 2020